Spectral Methods in Causal Dynamical Triangulations

Giuseppe Clemente
giuseppe.clemente@pi.infn.it

Talk based on the paper 1804.02294, written in collaboration with Massimo D'Elia (massimo.delia@unipi.it)

Istituto Nazionale di Fisica Nucleare
Università di Pisa

New frontiers in theoretical physics XXXVI
Cortona, 25 May 2018

Overview

The QG problem

Manifest difficulties:

- Standard perturbation theory fails divergences arise at short scale
- Gravitational quantum effects unreachable on lab: $E_{Pl} = \sqrt{\frac{\hbar c}{G}} c^2 \simeq 10^{19} GeV$ (big bang or black holes)

Two lines of direction in QG approaches

- non-conservative: introduce new short-scale physics
- conservative: do not give up on the Einstein theory

Causal Dynamical Triangulations (CDT): conservative approach of non-perturbative renormalization of the Einstein gravity via Monte-Carlo simulations.

Lattice regularization

A *regularization* makes the renormalization procedure well posed.

- discretize spacetime introducing a minimal **lattice spacing** ‘a’
- localize dynamical variables on lattice sites
- study how quantities diverge for $a \to 0$
- Cartesian grids approximate Minkowski space
- **Regge triangulations** approximate generic manifolds

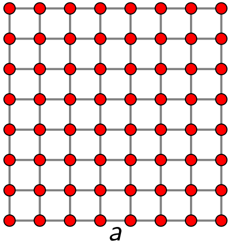

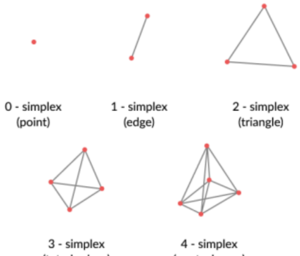

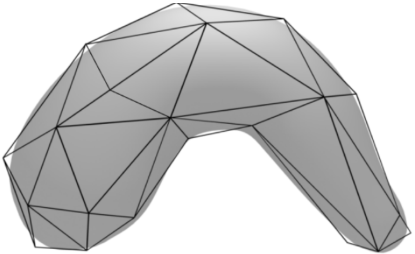

Regge formalism: action discretization

Also the EH action must be discretized accordingly ($g_{\mu\nu} \to \mathcal{T}$):

$$S_{EH}[g_{\mu\nu}] = \frac{1}{16\pi G}\left[\underbrace{\int d^d x\,\sqrt{|g|}\,R}_{\text{Total curvature}} - 2\Lambda \underbrace{\int d^d x\,\sqrt{|g|}}_{\text{Total volume}}\right]$$

$$\Downarrow \qquad \text{discretization} \qquad \Downarrow$$

$$S_{Regge}[\mathcal{T}] = \frac{1}{16\pi G}\left[\sum_{\sigma^{(d-2)}\in\mathcal{T}} 2\varepsilon_{\sigma^{(d-2)}} V_{\sigma^{(d-2)}} - 2\Lambda \sum_{\sigma^{(d)}\in\mathcal{T}} V_{\sigma^{(d)}}\right],$$

where $V_{\sigma^{(k)}}$ is the k-volume of the simplex $\sigma^{(k)}$.

Wick-rotation $iS_{Lor}(\alpha) \to -S_{Euc}(-\alpha)$

$\implies$ Monte-Carlo sampling $\mathcal{P}[\mathcal{T}] \equiv \frac{1}{Z}\exp\left(-S_{Euc}[\mathcal{T}]\right)$

Wick rotated action in 4D

At the end of the day [Ambjörn et al., arXiv:1203.3591]:

$$S_{CDT} = -k_0 N_0 + k_4 N_4 + \Delta(N_4 + N_4^{(4,1)} - 6N_0)$$

- New parameters: (k_0, k_4, Δ), related respectively to G, Λ and α.
- New variables: N_0, N_4 and $N_4^{(4,1)}$, counting the total numbers of vertices, pentachorons and type-$(4,1)/(1,4)$ pentachorons respectively ($\mathcal{T}$ dependence omitted).

It is convenient to "fix" the total spacetime volume $N_4 = V$ by fine-tuning $k_4 \implies$ actually free parameters (k_0, Δ, V).

Simulations at different volumes V allow finite-size scaling analysis.

Ultimate goal

Find a second order critical point in the phase diagram
$\Longrightarrow$ **renormalize the theory**.

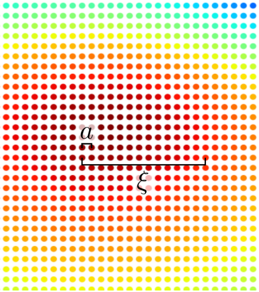

Continuum limit

The system must forget the lattice discreteness: second-order critical point with divergent correlation length $\hat{\xi} \equiv \xi/a \to \infty$

Asymptotic freedom (e.g. QCD):

$$\vec{g}_c \equiv \lim_{a\to 0} \vec{g}(a) = \vec{0}$$

Asymptotic safety (maybe QG):

$$\vec{g}_c \equiv \lim_{a\to 0} \vec{g}(a) \neq \vec{0}$$

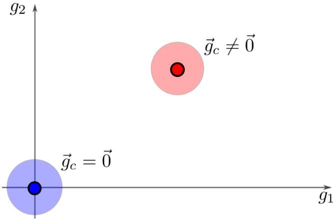

Phase diagram of CDT in 4D

k_4 "tuned" to fix $V \implies$ remaining free parameters: (k_0, Δ)

phase	spatial volume per slice
A:	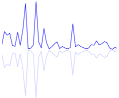
B:	
C_{dS}/C_b:	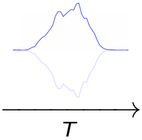

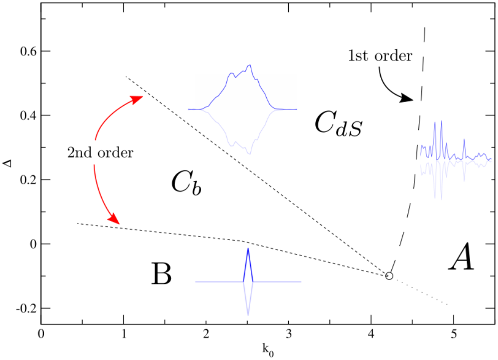

possible 2nd order lines have been found [1108.3932,1704.04373]
C_b and C_{dS} differ by the geometry of slices (discussed later)

Problem: lack of observables

A proper investigation of the continuum limit should require a possibly complete set of geometric observables.

Observables currently employed in CDT

- Spatial volume per slice: $V_s(t)$
  (number of spatial tetrahedra at the slice labeled by t)
- Order parameters for transitions:
  - $\text{conj}(k_0) = N_0/N_4$ for the $A|C_{dS}$ transition
  - $\text{conj}(\Delta) = (N_4^{(4,1)} - 6N_0)/N_4$ for the $B|C_b$ transition
  - OP_2 for the $C_b|C_{dS}$ transition
    [Ambjorn et al. arXiv:1704.04373]
- Fractal dimensions: (actually give some info at different scales)
  - spectral dimension
  - Hausdorff dimension

No observable characterizing geometries at all lattice scales!!

spectral methods

Hearing the shape of a manifold

- Spectral analysis on smooth manifolds $(\mathcal{M}, g_{\mu\nu})$:

$$-\nabla^2 f \equiv -\frac{1}{\sqrt{|g|}}\partial_\mu(\sqrt{|g|}g^{\mu\nu}\partial_\nu f) = \lambda f, \text{ with boundary conditions}$$

Can one hear the shape of a drum?

Almost: beside spectra you need also eigenvectors.

Example:
disk drum

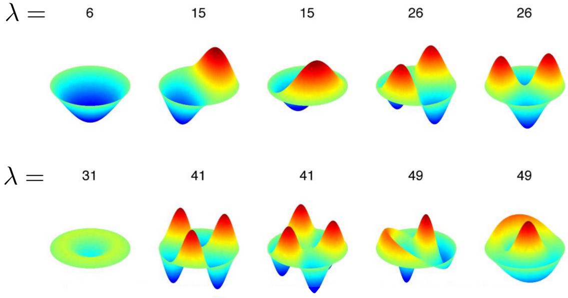

Spectral graph analysis of CDT slices

Observation

Spatial slices in CDT are made by identical $(d-1)$-simplexes
$\Longrightarrow$ a d-regular undirected graph is associated to any spatial slice.

- Spatial tetrahedra become vertices of associated graph
- Adjacency relations between tetrahedra become edges
- Laplace matrix: $L = D - A$, where $D = d\mathbb{1}$ is the *degree matrix* and A is the *adjacency matrix*.
- Eigenvalue problem $L\vec{f} = \lambda\vec{f}$ solved by numerical routines

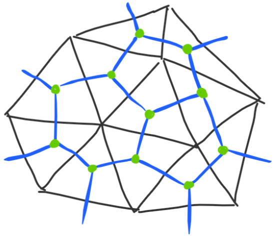

2D slice and its dual graph

Physical interpretation of LB eigenvalues and eigenvectors

Heat/diffusion equation on a manifold (or graph) M:

$$\partial_t u(x;t) - \Delta u(x;t) = 0\,.$$

General solution in a basis $\{e_n\}$ of LB eigenvectors ($\lambda_n \leq \lambda_{n+1}$):

$$u(x;t) = \sum_{n=0}^{|\sigma_M|-1} e^{-\lambda_n t}\widetilde{u}_n(0)e_n(x)\,.$$

consequences:

- λ_n is the diffusion rate for the (eigen)mode $e_n(x)$
- smallest eigenvalues $\leftrightarrow$ slowest diffusion directions.
- a large **spectral gap** λ_1 implies a fast overall diffusion, geometrically meaning a highly connected graph.

Weyl's law and effective dimension

For a manifold M with LB spectrum σ_M define:
$n(\lambda) \equiv \sum_{\bar{\lambda} \in \sigma_M} \theta(\bar{\lambda} - \lambda) =$ "number of eigenvalues below λ".

Weyl's law

Well known asymptotic result from spectral geometry:

$$n(\lambda) \sim \frac{\omega_d}{(2\pi)^d} V \lambda^{d/2} ,$$

being ω_d the volume of a unit d-ball and V the manifold volume.

Motivated by Weyl's law we define the **effective dimension**:

$$d_{EFF}(\lambda) \equiv 2 \frac{d \log(n/V)}{d \log \lambda} .$$

A toy model: toroidal lattice

Consider a 3-d periodic lattice with sizes $L_x \times L_y \times L_z$.

eigenvalues:

$$\lambda'_{\vec{m}} = 4\pi^2 \left(\frac{m_x^2}{L_x^2} + \frac{m_y^2}{L_y^2} + \frac{m_z^2}{L_z^2} \right) ,$$

with $m_i \in (-L_i/2, L_i/2] \cap \mathbb{Z}$.

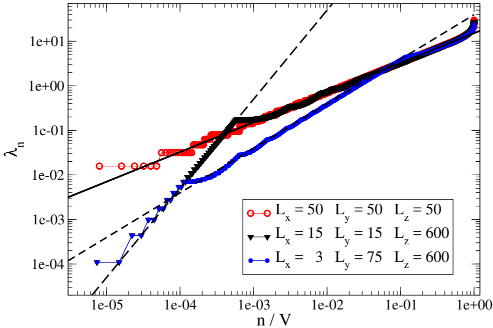

- Three regimes observed for $L_x \ll L_y \ll L_z$ with $d_{EFF} = 1, 2, 3$.
- Position of knees related to the scale of dimensional transition.

numerical results

Numerical simulations of 4D CDT

Simulations performed for total spatial volumes $N_{3s} = 20k, 40k$

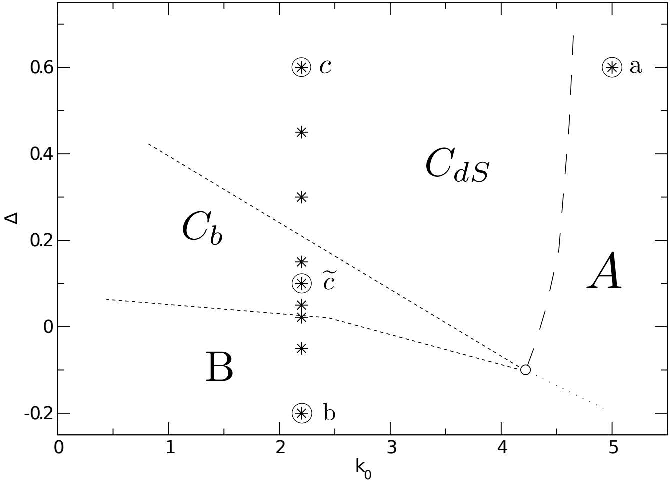

Spectral gap in different phases

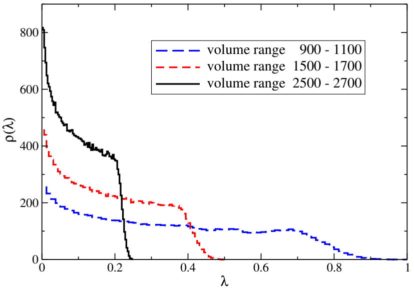

C_{dS} phase (first 100 eigenvalues)

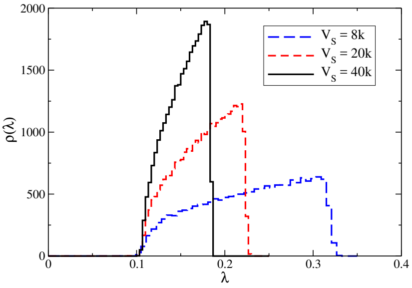

B phase (first 100 eigenvalues)

- no spectral gap in C_{dS} phase.
- non-zero spectral gap for slices in B phase (high connectivity).
- some volume dependence is present (except for λ_1 in B phase)

Collapse of scaling curves

The volume dependence can be reabsorbed by mapping λ_n vs n/V
$\Longrightarrow$ curves collapse into a volume independent function.

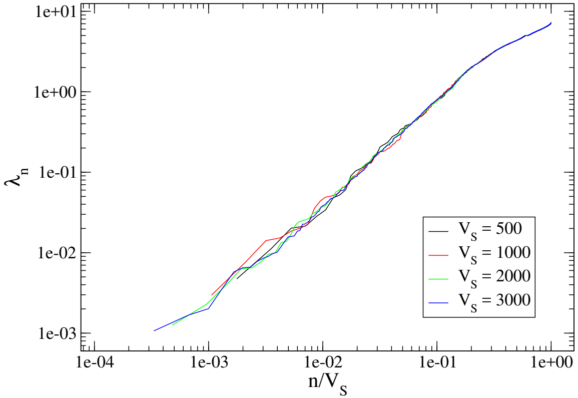

Weyl scalings for few slice in C_{dS} phase and different volumes

Scalings for different phases

By averaging over many slices (C_b discussed later):

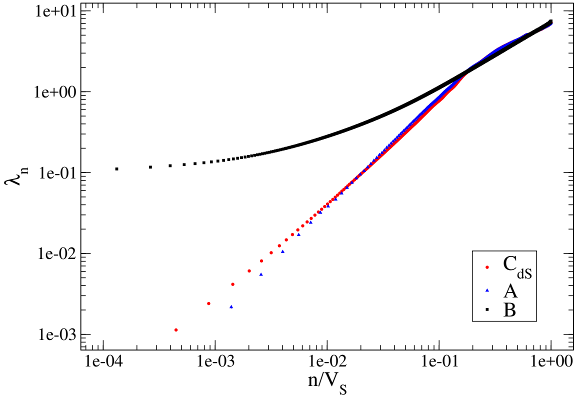

small λ (large scale) behaviour:

- vanishing spectral gap and finite slope for C_{dS} and A phases
- non-zero spectral gap and vanishing slope for B phase

Effective dimension for different phases

From the previous curves and the definition of **effective dimension**: $d_{EFF} \equiv 2\frac{d\log(n/V)}{d\log\lambda}$.

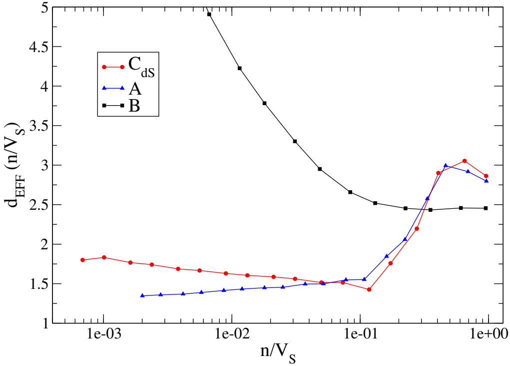

- $d_{EFF} \to \infty$ at large scales for B phase
- $d_{EFF} < 3$ for C_{dS} (and A) phase! $\implies$ fractional dimension

The bifurcation phase C_b

Similarities with C_{dS}:

- configurations with time extended blob
  (but narrower w.r.t. C_{dS} ones with the same k_0)
- similar spatial volume per slice $V_s(t)$

Main distinguishing feature (as known from previous literature):

- two classes of spatial slices, alternated in slice time, one of which possesses vertices with very high coordination number.

$\Longrightarrow$ Order parameter of C_b-C_{dS} transition defined in literature as relative difference between maximal coordination numbers of vertices in adjacent slices.

Alternating spectra in C_b configurations

Comparisons between C_{dS} and C_b low lying spectra:

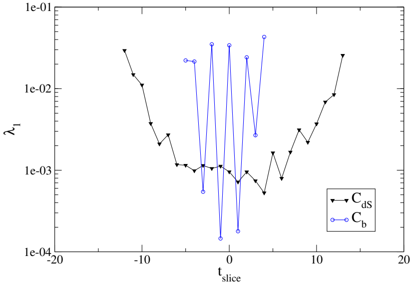

spectral gap for single configurations

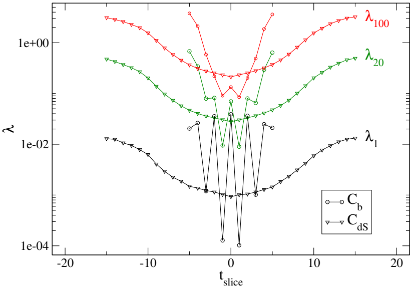

selected eigenvalues averaged over many configurations

The low lying spectra capture well the alternating behaviour of slice geometries in C_b configurations, and show it is a difference in large scale properties of slices.

Bifurcated scaling and class separation in C_b phase

Not a single scaling curve for C_b configurations
$\Longrightarrow$ a separation into two classes of slices is required:

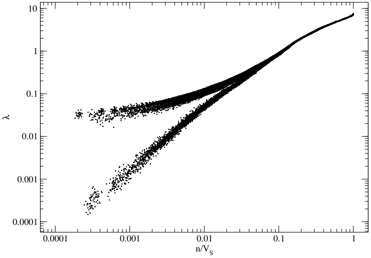

scatter plot λ vs n/V

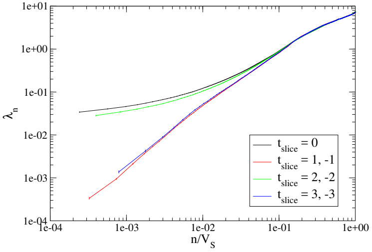

averaged values for different classes

We called the classes B-type and dS-type (for obvious reasons).

Spectral gap through phases

Spectral gap histogram for simulations with $k_0 = 2.2$ and different Δ:

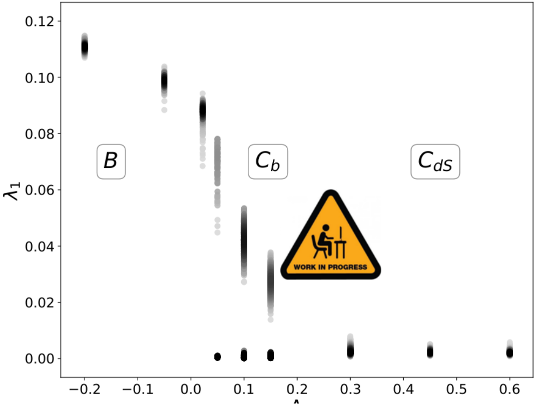

We are currently investigating the continuum limit around C_{dS}-C_b.

Conclusions

Results up to now:

- spectral gap characterizes connectivity in different phases
- Weyl's scaling allow to define a running effective dimensionality
- full spectral densities show non-trivial and interesting features (not shown here)

Future work:

- generalize to full spacetime configurations (FEM methods required)
- apply to EDT configurations ("straightforward")
- analyze all the features of eigenvectors (possessing the remaining information about the geometry), i.e. Anderson localization, Morse analysis, etc...
- investigate continuum limit (currently work in progress)